4144 *Inorg. Chem.* **1986**, *25*, 4144–4152

Contribution from the Laboratoire de Chimie Moléculaire, Unité Associée au CNRS, Université de Nice, 06034 Nice, France, and Laboratoire de Chimie Organique Physique, LA 321, Université Scientifique et Médicale, Département de Recherches Fondamentales, Centre d'Etudes Nucléaires 85X, 38041 Grenoble, France

Coordination Chemistry of the Bicycloaminophosphorane $Ph(H)P[(OCH_2CH_2)_2N]$, a Potential P/N Ligand. Access to Iron and Ruthenium Phosphoranides. Reversible Migration of a Phenyl Group between Iron and Phosphorus: Crystal and Molecular Structure of η^5-CpFe(CO)[P(OCH$_2$CH$_2$)$_2$N](η^1-C$_6$H$_5$)

Pierre Vierling,[†] Jean G. Riess,*[†] and André Grand[‡]

Received December 18, 1985

The bicyclic aminophosphorane **1**, in its open tautomeric form **1′**, behaves toward η^5-CpFe(CO)$_2$X (X = Cl, Br) mainly as a P-bonded monodentate ligand by displacement of X, and as a P/N bidentate ligand by replacement of CO and X, to yield the cationic derivatives **8a,b,d** and **10a,b,d**, respectively. With η^5-CpRu(CO)$_2$Cl, only the latter behavior is observed, leading to the cationic complex **10c**. In solution, the P/N chelates **10** are in equilibrium with the isomeric neutral derivatives **9**, as a result of competition between N and X for coordination to the metal. Abstraction of the N-borne proton by LiMe in the cationic chelates **11** leads quantitatively to the first iron and ruthenium phosphoranide adducts **13**. In the case of ruthenium, prior formation of the amido–phosphane chelate **12c** is observed. The iron species **13b,d** convert, under heating, into the iron η^1-phenyl derivatives **15b,d** as a result of migration of the phenyl group from phosphorus to iron, with concomitant conversion of the phosphoranide ligand into a phosphane ligand. Adduct **15b**, $C_{16}H_{18}FeNO_3P$, crystallizes in the monoclinic space group $P2_1/n$, with $a = 7.776$ (1) Å, $b = 14.477$ (3) Å, $c = 14.083$ (1) Å, $\beta = 102.04$ (1)°, and $Z = 4$. The Fe–C(Ph) (2.037 (5) Å), Fe–C(CO) (1.715 (5) Å), and Fe–P (2.105 (3) Å) bond lengths are among the shortest distances known for complexes of this type. The P–N bond is also remarkably short (1.692 (4) Å) in spite of the fact that the nitrogen atom is markedly pyramidal ($\sum_N = 333 \pm 9.0°$). The phenyl group migration is quantitatively reversed from iron back to phosphorus under the action of gaseous HCl. Chemical labeling of the phenyl ring excludes an ortho-metalation pathway and shows that it is the same carbon atom that is bonded alternately to phosphorus and to iron, establishing a 1,2-sigmatropic shift mechanism for this reversible phenyl migration. Furthermore, this phenomenon exemplifies (i) a metal-induced interconversion between a hypervalent P(V) phosphorane (**1**) and a trivalent P(III) phosphane derivative (**17**) and (ii) the possible intermediate formation of phosphoranide adducts in P–C bond rupture processes.

Introduction

The bicyclic aminophosphorane **1** is the precursor of a multi-donor-site ligand in both its open, monocyclic and its closed, bicyclic tautomeric forms. The former coordinates transition metals[1] either via the phosphorus atom (as in **3**) or via both phosphorus and nitrogen atoms (as in **4**). More recently the latter was found to be present in the novel type of transition metal compounds **6**[2] and **7**,[3] the first to contain a phosphoranide ligand, the first also in which the metal bridges a P–N or a P–O bond to form the following previously unknown metallacycles:

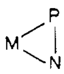

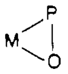

The transition-metal amide **5**[4] has also been obtained recently.

In order to extend these new families of compounds and to further explore the coordinating ability of the versatile ligands of type **1**, we investigated the action of **1** on η^5-CpFe(CO)$_2$X (X = Cl or Br) and the abstraction of the nitrogen-bonded proton from iron analogue **11b** of **4**, with the aim of obtaining either phosphoranides analogous to **6** or **7** or amides analogous to **5**.

To our surprise neither a phosphoranide nor an amide derivative could be isolated. Instead, a new reaction was observed to occur, which led to compound **15b**, as reported in a preliminary communication:[5] under the action of the base, we observed the migration of the phenyl group from phosphorus to iron, with concomitant conversion of the bidentate monocyclic ligand into a monodentate bicyclic one. Also surprising was the observation that this migration is *reversible*: the action of an acid converts adduct **15b** back to **11b**, smoothly and quantitatively. This interconversion between **11b** and **15b**, which is in fact the metal-induced interconversion between a P(V) and a P(III) species, i.e. between **1** and **17**, appears to be an original feature in phosphorus chemistry.

We have now investigated the mechanism of this reversible phenyl group migration, and report a closer analysis of the sequence of reactions involved, as well as a detailed X-ray analysis of **15b**. The behavior of **11c**, the ruthenium analogue of **11b**, toward LiMe, was also investigated. This reaction produced an amide intermediate, **12c**, followed by a ruthenium phosphoranide complex, **13c**, but in contrast to the iron analogue, no phenyl migration reaction was observed.

Scheme I. Access to the Mo and W Phosphoranide Adducts **6** and **7**

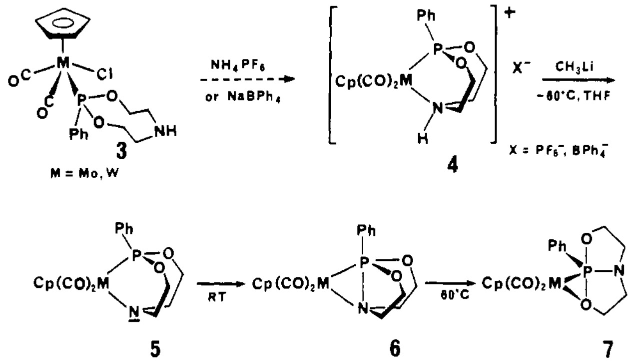

Results and Discussion

Ambidentate Behavior of the Bicyclic Aminophosphorane 1. Iron Derivatives. The coordination and organometallic chemistry of the η^5-CpFe(CO)$_2$X (X = halogen) derivatives has been extensively studied. Controlled replacement of one or both carbonyl

---

[†] Université de Nice.

[‡] Université Scientifique et Médicale de Grenoble.

(1) (a) Bondoux, D.; Tkatchenko, I.; Houalla, D.; Wolf, R.; Pradat, C.; Riess, J. G.; Mentzen, B. F. *J. Chem. Soc., Chem. Commun.* **1978**, 1022. (b) Pradat, C.; Riess, J. G.; Bondoux, D.; Mentzen, B. F.; Tkatchenko, I.; Houalla, D. *J. Am. Chem. Soc.* **1979**, *101*, 2234. (c) Wachter, J.; Jeanneaux, F.; Riess, J. G. *Inorg. Chem.* **1980**, *19*, 2169. (d) Wachter, J.; Mitschler, A.; Riess, J. G. *J. Am. Chem. Soc.* **1983**, *103*, 2121. (e) Bondoux, D.; Mentzen, B. F.; Tkatchenko, I. *Inorg. Chem.* **1981**, *20*, 839. (f) Mordenti, L.; Roustan, J. L.; Riess, J. G. *Organometallics* **1983**, *2*, 843.

(2) Jeanneaux, F.; Grand, A.; Riess, J. G.; *J. Am. Chem. Soc.* **1981**, *103*, 4272.

(3) Wachter, J.; Mentzen, B. F.; Riess, J. G. *Angew. Chem., Int. Ed. Engl.* **1981**, *20*, 284.

(4) Jeanneaux, F.; Grand, A.; Riess, J. G., unpublished results.

(5) Vierling, P.; Grand, A.; Riess, J. G. *J. Am. Chem. Soc.* **1981**, *103*, 2466.

0020-1669/86/1325-4144$01.50/0

Scheme II. Coordination Chemistry of **1** and **2** toward η^5-CpM(CO)$_2$X (M = Fe, Ru)

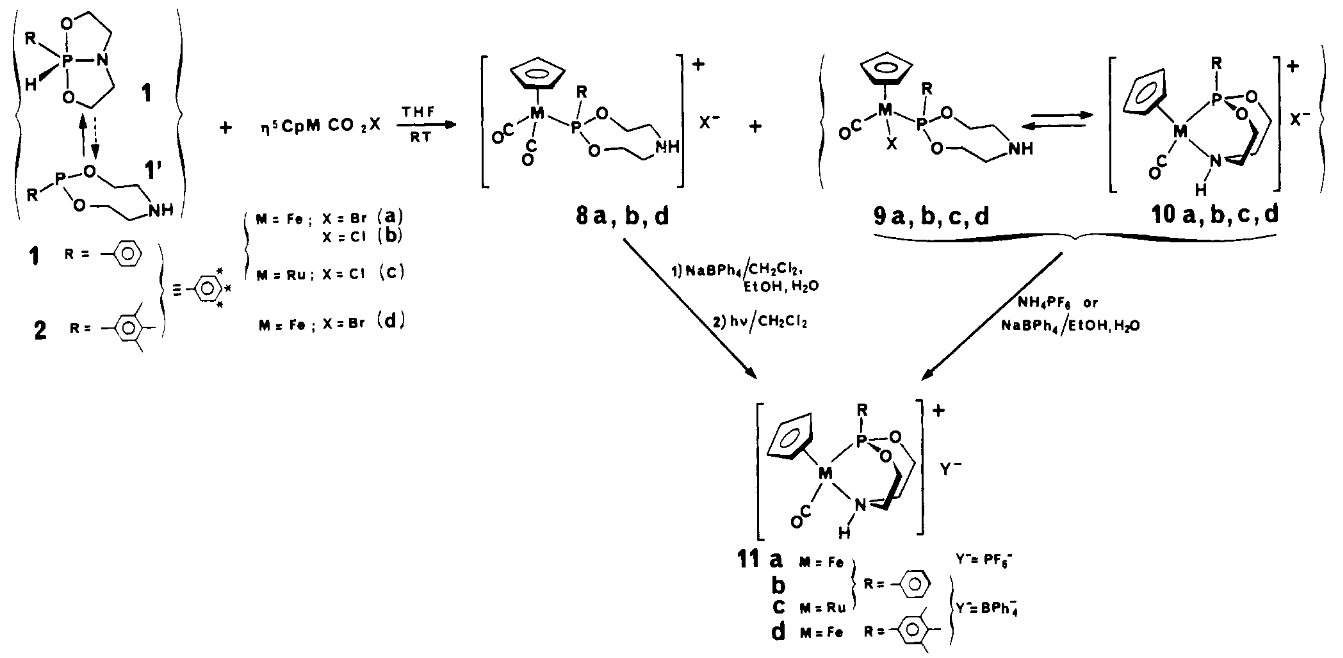

groups and of the halogen can be achieved, enabling a wide range of neutral and cationic cyclopentadienyl complexes to be prepared. Although the reactions of numerous monodentate[6-10] and multidentate[6c,9,11-13] ligands with η^5-CpFe(CO)$_2$X have been reported, only one report of a reaction of a mixed bidentate ligand, namely Ph$_2$PCH$_2$CH$_2$S$^-$Na$^+$, has appeared.[14] This reaction gives rise to displacement of halide and CO to form η^5-CpFe(CO)-Ph$_2$PCH$_2$CH$_2$S. No data involving a bidentate mixed P/N ligand are available so far, to our knowledge.

A rather complex situation was found when η^5-CpFe(CO)$_2$X (X = Cl, Br) was allowed to react with **1**. In THF at room temperature, a cream-colored precipitate formed, which was isolated in 65% yield and identified as **8a,b**. It results from the displacement of the halogen on iron and coordination of the phosphorus atom only of the open tautomeric form **1'** of **1**. Compounds **8a,b** are characterized by their IR spectra, which show two ν_{CO} bands of equal intensity (characteristic of all η^5-CpFe(CO)$_2$L$^+$X$^-$ compounds)[6c] at 2050 and 2000 cm^{-1} and a ν_{NH} vibration at 3400 cm^{-1} of low intensity characteristic of a noncoordinated nitrogen atom (a ν_{NH} at 3400 cm^{-1} is also found for **3**[1c]). The phosphorus–metal bond is supported by ^{31}P NMR (δ(^{31}P) = 180 in CH$_2$Cl$_2$ for both X = Cl and X = Br).

A second, red-brown, compound was isolated in 10–30% yield from the filtrate after separation of **8a,b** and was identified as **10a,b**. This is attested by the IR spectra (KBr), which show a single ν_{CO} stretch at 1940 cm^{-1} for X = Cl and 1945 cm^{-1} for X = Br and a single sharp and relatively intense ν_{N-H} stretch at 3300 cm^{-1} for both X = Cl and X = Br. This ν_{NH} band, shifted by 100 cm^{-1} toward lower frequencies with respect to the ν_{NH} of **8a,b**, indicates that the nitrogen atom is coordinated to iron.

A third (neutral) compound, **9a,b**, was found to be in equilibrium with **10a,b** in solution as a result of the competition of Br$^-$ (or Cl$^-$) with the NH site for coordination to iron. Thus the ^{31}P and ^{1}H NMR spectra of a saturated CD$_2$Cl$_2$ solution of **10a** for example exhibit, in a 2/3 ratio, two resonances at 210 and 196 ppm, and two doublets at 5.0 and 4.5 ppm ($^3J_{HP}$ = 1.2 Hz), for the Cp's protons, respectively; after Br$^-$ vs. PF$_6^-$ anion exchange and extraction of NH$_4$Br in the D$_2$O phase, only the downfield signals corresponding to the ionic structure **10a** (PF$_6^-$) are observed. The coupling constants $^3J_{HP}$ confirm that coordination of the phosphorus atom to the metal is preserved in **9** and **10**.

The major objective of this work being to explore the possibility of obtaining iron and ruthenium phosphoranides, it was desirable to have as a starting material a single, cationic, species in which **1'** would behave as a bidentate ligand. In order to achieve this and to prevent the equilibrium between **9** and **10**, we prepared **11a,b**, which were obtained nearly quantitatively from a solution of **10a,b** and NH$_4$PF$_6$ or NaBPh$_4$ in an ethanol/water mixture. The spectral characteristics of **11a,b** are very close to those measured for the Mo and W analogues **4**, whose structure has been confirmed by X-ray analysis in the case of **4** (M = Mo, X = PF$_6^-$).[15]

When performed under UV irradiation in toluene, the action of **1** on η^5-CpFe(CO)$_2$Br, causes (i) a significant increase in the reaction rate, with total consumption of the starting material in about 1 h instead of 2 days and (ii) a slight increase in the proportion of **10a** formed at the expense of **8a**. When ligand **2** reacts with η^5CpFe(CO)$_2$Br, a lower yield (12%) of **10d** (which was directly converted into and fully characterized as **11d**) was obtained along with 60% of **8d**. The yield of **10d** could not be improved under UV irradiation, which led us to investigate the possibility of converting the P-coordinated adduct **8** into the P- and N-coordinated complexes **10** or **11**. The coordination of the NH site, leading to **11b** (or **11d**) could be forced under UV irradiation of a CH$_2$Cl$_2$ solution of **8a,b** (or **8d**), provided the Cl$^-$ or Br$^-$ anions had first been exchanged with BPh$_4^-$ to prevent Arbusov-type reactions such as those observed when phosphite ligands react with η^5-CpFe(CO)$_2$X.[6a]

---

[6] (a) Haines, R. J.; Du Preez, A. L.; Marais, I. L. *J. Organomet. Chem.* **1971**, *28*, 405. (b) Davidson, A.; Green, M. L. H.; Wilkinson, G. *J. Chem. Soc.* **1961**, 3172. (c) Treichel, M. P.; Shubkin, R. L.; Barnett, R. W.; Reichard, D. *Inorg. Chem.* **1966**, *5*, 1177. (d) Treichel, M. P.; Komar, D. A. *J. Organomet. Chem.* **1981**, *206*, 77.

[7] Brown, D. A.; Lyons, H. J.; Manning, A. R.; Rowley, J. M. *Inorg. Chim. Acta* **1969**, *3*, 346; **1970**, *4*, 428.

[8] (a) King, R. B. *Inorg. Chem.* **1963**, *2*, 936. (b) King, R. B.; Gimeno, J. *Inorg. Chem.* **1978**, *17*, 2396.

[9] Tripathi, S. C.; Srivastava, S. C.; Pandey, V. N. *Transition Met. Chem.* (*Weinheim, Ger.*) **1976**, *1*, 266.

[10] Tripathi, S. C.; Srivastava, S. C.; Pandey, V. N. *Transition Met. Chem.* (*Weinheim, Ger.*) **1976**, *1*, 58.

[11] (a) Sellmann, D.; Kleinschmitt, E. *Angew. Chem., Int. Ed. Engl.* **1975**, *14*, 571. (b) Sellmann, D.; Kleinschmitt, E. *J. Organomet. Chem.* **1977**, *140*, 211.

[12] Haines, R. J.; Du Preez, A. L. *Inorg. Chem.* **1972**, *11*, 330.

[13] (a) King, R. B.; Houk, L. W.; Pannel, K. H. *Inorg. Chem.* **1969**, *8*, 1043. (b) King, R. B.; Kapoor, P. N.; Kapoor, R. N. *Inorg. Chem.* **1971**, *10*, 1841. (c) Treichel, P. M.; Molzahn, D. C. *Synth. React. Inorg. Met.-Org. Chem.* **1979**, *9*, 21. (d) King, R. B.; Kapoor, P. N.; Kapoor, R. N.; Saran, M. S. *Inorg. Chem.* **1971**, *10*, 1851, 1861.

[14] Savignac, M.; Cadiot, P.; Mathey, F. *Inorg. Chim. Acta* **1980**, *45*, L43.

[15] Wachter, J.; Mentzen, B. F.; Riess, J. G., unpublished results.

In conclusion, compound **1** in its open tautomeric form **1′**, behaves toward η^5-CpFe(CO)$_2$X primarily as a monodentate ligand through its phosphorus site by substitution of either the halide, leading to compound **8**, or of one CO group, leading to **9**, the former mode of substitution being favored. Nevertheless, a bidentate behavior is observed in **10**, either (i) by expulsion of the halide anion in **9**, which is present only in solution and in equilibrium with **10**, or (ii) by forced expulsion of a CO ligand under UV irradiation starting from **8**. These results differ from those observed when **1** reacts with the Mo and W analogues η^5-CpM(CO)$_3$Cl, in several aspects. In the latter case, three points are observed: (i) substitution of CO appears to occur exclusively to yield compounds **3**; (ii) these are covalent, and no equilibrium with the ionic structure **4** was detected in solution, the latter being observed to form only after Cl$^-$/PF$_6^-$ (or BPh$_4^-$) anion exchange had been made; (iii) coordination of the nitrogen atom by replacement of a CO ligand is easily realized, starting from **3**, under mild thermal conditions.[1c]

Ruthenium Derivatives. Most cyclopentadienyl–ruthenium chemistry has been investigated by starting from η^5-CpRu(PPh$_3$)$_2$Cl, which is easily prepared, where PPh$_3$ and/or Cl$^-$ ligands can readily be replaced by other ligands.[16,17] Chemistry based on η^5-CpRu(CO)$_2$X compounds has been less developed than that of the analogous iron derivatives. The reaction of phosphine and phosphite ligands L with η^5-CpRu(CO)$_2$X (X = Cl, Br, I) has long been reported to yield only carbonyl-substituted η^5-CpRu(CO)LX compounds.[18] More recently, however, two reports have shown that, in the presence of PEt$_3$[19] or PMe$_3$,[16a] the ionic halogen-displaced [η^5-CpRu(CO)$_2$L]$^+$Cl$^-$ derivatives are also formed. Halogen substitution in η^5-CpRu(CO)$_2$Cl is also achieved under the action of an amine (e.g. NH$_3$),[19] and the reaction of dppe (Ph$_2$PCH$_2$)$_2$ with η^5-CpRu(CO)$_2$Cl has been shown to yield the carbonyl and chloride-substituted [η^5-CpRu(CO)(dppe)]$^+$Cl$^-$.[19] Other monocarbonyl species were obtained by other routes, e.g. by carbonylation of η^5-CpRuL$_2$Cl.[16,17] To our knowledge, the action of bidentate P/N ligands toward η^5-CpRu(CO)$_2$Cl has not yet been investigated.

The reaction of **1** with η^5-CpRu(CO)$_2$Cl leads quantitatively to the stable ionic compound **10c**. Its infrared spectrum (one ν_{CO} band at 1945 cm^{-1} (KBr)) is consistent with carbonyl displacement through P-coordination, and a sharp ν_{NH} stretch at 3320 cm^{-1} implies that N-coordination has occurred too. On the other hand, the ^{1}H and ^{31}P NMR spectra show, as observed for iron (vide supra), that both the covalent **9c** and the ionic **10c** forms are present in solution. The ^{31}P and ^{1}H NMR spectra of a saturated CDCl$_3$ solution exhibit, respectively and in a 35/65 ratio, two resonances at 183 and 167 ppm and two doublets for the Cp protons, at 5.44 ppm ($^3J_{HP}$ = 0.6 Hz) and 5.0 ppm ($^3J_{HP}$ = 0.9 Hz); the coupling constants $^3J_{HP}$ are consistent with P-coordination to ruthenium. The downfield signals were assigned to the ionic isomer **10c** on the grounds that only the signals attributed to **10c** (PF$_6^-$) were detected after a Cl$^-$/PF$_6^-$ anion exchange.

The behavior of **1** toward η^5-CpRu(CO)$_2$Cl deserves comment. In the case of bidentate P/P ligands (e.g. dppm = Ph$_2$PCH$_2$PPh$_2$ and dppe), the coordination of the second donor site on the metal center was shown to occur either by displacement of a second CO, as illustrated by the loss of CO in the unstable η^5-CpRu(CO)(dppm)Cl, yielding η^5-CpRu(dppm)Cl,[17] or by displacement of chloride, as in the case of the stable ionic [η^5-CpRu(CO)(dppe)]$^+$Cl$^-$ derivative.[19] In the case of the cyclic P/N ligand **1′**, the initial coordination of the phosphorus atom in **9c** is followed by a competition between Cl$^-$ and N for coordination.

Scheme III. Access to the Fe and Ru Phosphoranide Adducts. Reversible Phenyl Migration between **11b,d** and **15b,d** which Illustrates the Metal-Induced **1** ⇌ **17** Interconversion

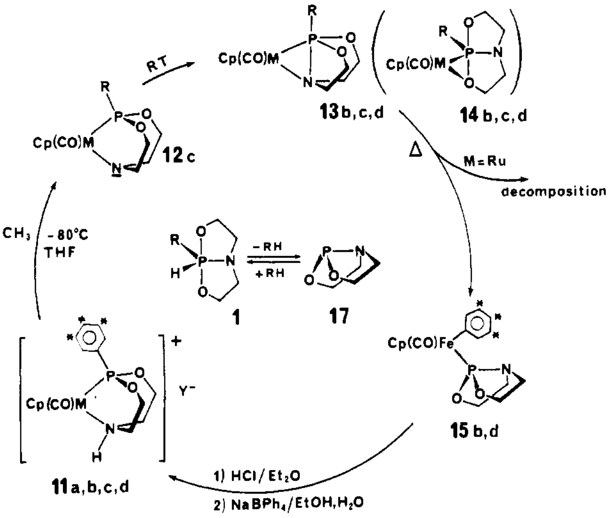

Synthesis and Characterization of the First Iron and Ruthenium Phosphoranide Adducts. The ionic complexes **11** were synthesized in view of studying the abstraction of the nitrogen-bonded hydrogen atom by a base, with the aim of obtaining metal phosphoranide complexes. In this approach the formation of **11** was expected to serve both as a straightforward way of forming the P–M bond and as a relay to facilitate the abstraction of the proton initially located on phosphorus in **1**. Such an intramolecular–intraligand approach proved effective indeed in the synthesis of the first transition-metal phosphoranides **6**[2] and **7**,[3] and also of metal cyclamphosphoranides.[20] More recently, other routes to transition-metal-substituted phosphoranes have been described.[21]

Under the action of LiMe in THF, the cationic iron derivatives **11b,d** are first converted quantitatively at −80 °C into the iron phosphoranides **13b,d**. The ν(CO) vibration of **11b,d** at 1965 cm^{-1} is seen to disappear, while a new absorption develops at 1910 cm^{-1}. Concomitantly, the low-field ^{31}P resonances at 209 ppm for **11b**, or at 208 ppm for **11d**, are replaced by upfield signals at 69 ppm in the first case, or at 74 ppm in the second, in the spectra immediately recorded at −100 °C. Increasing the temperature causes no change in the spectra apart from the expected shifts of the lines with temperature (to 73 and 80 ppm, respectively, at 20 °C). All attempts to isolate these adducts failed, however, owing to decomposition during the isolation procedure; complexes **13b,d** are stable in solution only at temperatures lower than 0 °C. The NMR-based structural assignments are discussed below.

The ruthenium cationic derivative **11c**, under the same conditions as above, is converted first into the yellow amido–phosphane adduct **12c**, which could be isolated in 90% yield. Its chemical shift (181 ppm) is very close to that measured for the cationic derivative **11c** (182 ppm in CH$_3$CN). However, that it is a different compound is definitely evidenced by its IR spectrum, which shows a ν_{CO} vibration at 1920 cm^{-1}, compared to 1970 cm^{-1} for **11c**. This amido–phosphane complex is unstable at room temperature, both in the solid state and in solution, and converts slowly into the ruthenium phosphoranide adduct **13c**. The two transformations can easily be monitored by ^{31}P NMR spectroscopy. When the addition of LiMe to **11c** in THF (in which **11c** is insoluble) is performed at −100 °C, a clear yellow solution, which is characterized by a ^{31}P resonance at 183 ppm, is obtained within

---

(16) (a) Treichel, P. M.; Komar, D. A. *Synth. React. Inorg. Met.-Org. Chem.* **1980**, *10*, 205. (b) Blackmore, R.; Bruce, M. I.; Stone, F. G. A. *J. Chem. Soc. A* **1971**, 2376. (c) Haines, R. J.; Du Preez, A. L. *J. Organomet. Chem.* **1975**, *84*, 357.

(17) Ashby, G. S.; Bruce, M. I.; Tomkins, I. B.; Wallis, R. C. *Aust. J. Chem.* **1979**, *32*, 1003.

(18) (a) Brown, D. A.; Lyons, H. J.; Sane, R. T. *Inorg. Chim. Acta* **1970**, *4*, 621. (b) White, C.; Tabatabarian, K. *Inorg. Chem.* **1981**, *20*, 2020. (c) Howell, J. A. S.; Rowan, A. J. *J. Chem. Soc., Dalton Trans.* **1980**, 1845.

(19) Jungbauer, A.; Behrens, H. *Z. Naturforsch, B: Anorg. Chem., Org. Chem.* **1978**, *33B*, 1083.

(20) Dupart, J. M.; Grand, A.; Pace, S.; Riess, J. G. *J. Am. Chem. Soc.* **1982**, *104*, 2316.

(21) (a) Lattman, M.; Anand, B. N.; Garret, D. R.; Whitener, M. A. *Inorg. Chim. Acta* **1983**, *76*, L139. (b) Ebsworth, E. A. V.; McManus, N. T.; Pilkington, J. J.; Rankin, D. W. H. *J. Chem. Soc., Chem. Commun.* **1983**, 484. (c) Lattman, M.; Morse, S. A.; Cowley, A. H.; Lasch, J. G.; Norman, N. C. *Inorg. Chem.* **1985**, *24*, 1364.

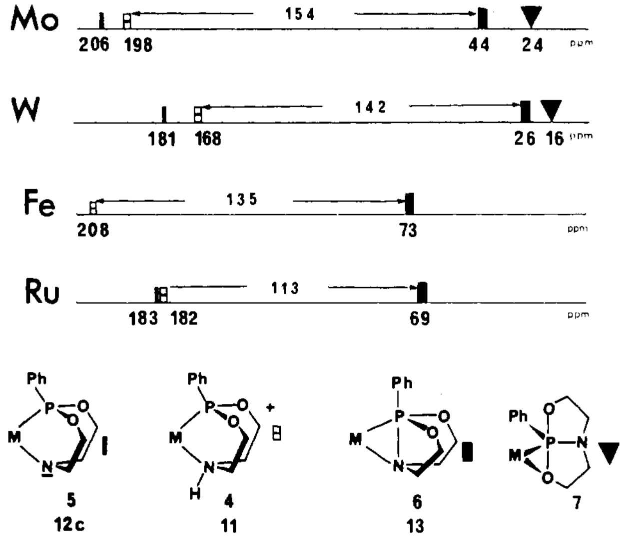

Figure 1. Variation ($\Delta\delta$) of the $\delta(^{31}P)$ NMR spectra for the transformations **4** → **5** → **6** → **7** and **11** → **12** → **13**.

minutes. Increasing the temperature to RT causes no line broadening (the ^{31}P signal is found at 182 ± 1 ppm throughout the entire temperature range and remains narrow). At room temperature, however, the THF solution slowly turns from yellow to yellow-orange. Simultaneously the low-field ^{31}P resonance is replaced by an upfield signal at 69 ppm. This transformation is completed within 12 h. This experiment establishes that formation of the amido–phosphane complex **12c** occurs prior to formation of the phosphoranide **13c**.

The structure assignments of **12c** and **13b,c,d** are mainly based on comparison of the ^{31}P NMR data[22] with those of the analogous Mo and W derivatives **5**,[4] **6**,[2] and **7**,[3] (Figure 1) whose structures have been confirmed by X-ray analysis. Infrared and ^1H NMR spectroscopies permit a clear distinction between the cationic derivatives on one hand and the amido–phosphane and phosphoranide adducts on the other, but not between the latter two types of complexes, since in both cases the carbonyl vibrations are shifted to low frequencies, and the ^1H signals of the cyclopentadienyl protons are shifted upfield with respect to the cationic starting complexes, as expected from an increase in the electron density at the metal. The amido–phosphane and the phosphoranide complexes can be distinguished unambiguously by ^{31}P NMR (figure 1): the formation of the former complex was found in the Mo and W series[4] to be accompanied by downfield variations in chemical shifts ($\Delta\delta$) of only −8 and −13 ppm for **5**, with respect to the cationic derivative **4**, the ^{31}P chemical shift thus staying, as expected, within the 160–220 ppm range characteristic of M(II)–phosphane adducts; the chemical shift (182 ppm) measured for the ruthenium derivative **12c** is also well within this range. On the other hand, a considerable upfield $\Delta\delta$ accompanies the formation of the Mo and W phosphoranides **6** with respect to the corresponding cationic adduct **4** ($\Delta\delta$ = 154[2] and 142[3] ppm, respectively). A similarly large upfield variation is found for the iron and ruthenium derivatives ($\Delta\delta$ = 135 and 113 ppm, respectively), therefore evidencing the formation of the phosphoranides **13** for these two metals. The fact that only one single line is present in the ^{31}P NMR spectra throughout the −100 to +20 °C temperature range for the iron and ruthenium phosphoranides points to the formation of only one of the two possible phosphoranides **13** and **14**. The latter appears less probable in view of the higher values of $\Delta\delta$ (174 and 152 ppm, respectively) that accompany the formation of the Mo and W phosphoranides **7**;[2,3] an exchange between isomers **13** and **14**, which may also involve the phosphoranide **14′** and which would already be rapid at −100 °C, can however not be completely ruled out. Increasing the temperature above 20 °C causes the migration of the phenyl group, in the case of the iron derivatives **13b,d**, and fast decomposition, in the case of the ruthenium adduct **13c**, thus precluding the detection of a possible isomerization **13** → **14**, as observed at higher temperatures for Mo and W.

Table I. Crystallographic Data for **15b**

formula:	$C_{16}H_{18}NO_3PFe$	recording temp:	20 °C
fw:	359.14	Mo Kα radiation:	λ = 0.7090 Å
monoclinic		scan rate:	2° min^{-1}
space group:	$P2_1/n$	θ range:	2° < θ < 25°
a =	7.776 (1) Å	octants recorded:	h,k,l; $-h,k,l$
b =	14.477 (3) Å	no. of data collcd:	2846
c =	14.083 (1) Å	no. of data $F_o \geq 2.5\sigma(F_o)$:	2000
β =	102.04 (1)°	cryst size:	0.15 × 0.15 × 0.2 mm
V =	1550.5 $Å^3$		
Z =	4		
$F(000)$ =	336	R_F =	0.057
μ =	10.673 cm^{-1}	R_{wF} =	0.035
d_{measd}/d_{calcd} =	1.52/1.539 g cm^{-3}		

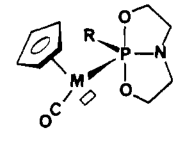

14′

Reversible Phenyl Group Migration Mechanism. Occurrence. Heating a THF solution of the iron phosphoranide **13b** results in the migration of the phenyl group from phosphorus to iron, leading to compound **15b**, which was isolated by chromatography on silica in 35% yield as amber crystals. That a redistribution of bonds had occurred is suggested by IR and ^1H, ^{31}P, and ^{13}C NMR spectroscopies. Thus the IR spectra of **15b** shows a ν_{CO} absorption at 1930 cm^{-1} and, for the phenyl group, a narrow and relatively intense $\nu_{C=C}$ absorption at 1560 cm^{-1}, while this vibration is found at 1580 cm^{-1} and is of very low intensity when the phenyl ring is bonded to phosphorus as in **11a**. The ^{31}P chemical shift at 217 ppm for **15b** agrees with a M(II)–phosphane adduct. Finally, the absence of coupling between the ^{13}C nuclei of the phenyl group and the ^{31}P nuclei strongly suggests that the phenyl ring is no longer bonded to phosphorus. An X-ray diffraction analysis was then undertaken, which definitely establishes the structure of the reaction product to be **15b** where the phenyl ring is now bonded to iron, while the phosphoranide ligand is converted into the bicyclic aminophosphane ligand **17**.

Surprisingly, this phenyl group migration can be *reversed* under the action of gaseous HCl on **15b**, which is then quantitatively converted to **11b**. This reversible phenyl group migration exemplifies a metal-induced interconversion between a phosphorane (**1**) and a phosphane (**17**), i.e. between a hypervalent P(V) and a normalvalent P(III) state.

In spite of cautious investigations, this phenomenon was not detected when similar conditions were applied to the ruthenium, molybdenum, and tungsten analogues.

X-ray Structure of the Phenyliron–Phosphane Adduct 15b. Figure 2 shows an Ortep representation of the molecule with the labeling scheme used, and Table III collects the bond distances and angles.

The geometric arrangement of the ligands around iron can be described as a distorted tetrahedron. With respect to η^5-$CpFe(CO)_3^+$,[23] where the angles between the carbonyl ligands are close to 90°, one finds 94.5° for C63–Fe–CO and 83.9° for C63–Fe–P. It is of particular interest to compare the crystal data of **15b** with those of the closely related PPh_3 derivative η^5-$CpFe(CO)(PPh_3)(\eta^1$-$Ph)$ (**20**).[24] The most striking difference is here that all bond distances around iron in **15b** are significantly shorter than the related ones in **20** (Table IV). This is in particular the case

---

(22) Riess, J. G. In *^{31}P NMR Spectroscopy—Structural and Stereochemical Investigation of Organic and Metal Complex Compounds*; Verkade, J. G., Quin, L., Eds.; Verlag Chemie: Weinheim, FRG, 1985.

(23) Gress, M. E.; Jacobson, R. A. *Inorg. Chem.* **1973**, *12*, 1746.

(24) Semion, V. A.; Sturchkov, Yu. T. *Z. Strukt. Khim.* **1969**, *10*, 88.

Table II. Atomic Coordinates and Anisotropic Thermal Parameters with Their Esd's ($\times 10^4$)

atom	x	y	z	β_{11}	β_{22}	β_{33}	β_{12}	β_{13}	β_{23}
Fe	3209 (1)	7156 (1)	5752 (1)	105 (1)	27 (1)	41 (1)	5 (1)	10 (1)	1 (1)
P	742 (2)	7693 (1)	5860 (1)	96 (2)	28 (1)	45 (1)	−3 (1)	19 (1)	0 (1)
N	185 (5)	8817 (3)	5660 (3)	104 (8)	33 (2)	54 (3)	9 (3)	2 (4)	2 (2)
O1	−900 (4)	7278 (2)	5074 (2)	102 (6)	45 (2)	77 (3)	−12 (3)	11 (3)	−16 (2)
O2	260 (4)	7612 (2)	6909 (2)	160 (8)	47 (2)	61 (3)	12 (3)	46 (3)	7 (2)
O3	2970 (4)	8034 (3)	3897 (3)	263 (10)	65 (3)	39 (2)	−35 (4)	3 (4)	8 (2)
CO	3068 (5)	7690 (3)	4652 (4)	101 (10)	37 (3)	42 (3)	−4 (4)	13 (4)	−4 (3)
C81	−2258 (6)	7969 (4)	4769 (4)	89 (10)	60 (4)	82 (5)	8 (5)	−18 (5)	−6 (4)
C82	−1288 (6)	8874 (4)	4820 (4)	127 (11)	54 (4	66 (4)	3 (5)	−16 (6)	15 (3)
C83	−77 (7)	9206 (4)	6585 (4)	162 (12)	51 (4)	83 (5)	26 (5)	37 (7)	−8 (4)
C84	−650 (7)	8437 (4)	7167 (4)	234 (14)	74 (4)	48 (4)	43 (7)	24 (6)	1 (4)
C61	4993 (7)	9044 (4)	8100 (4)	175 (12)	56 (4)	39 (4)	8 (6)	12 (5)	−9 (3)
C62	4353 (6)	8271 (3)	7550 (4)	128 (10)	43 (3)	35 (3)	4 (5)	5 (5)	0 (3)
C63	4155 (6)	8293 (3)	6543 (3)	99 (10)	31 (3)	42 (4)	4 (4)	−3 (5)	−8 (3)
C64	4596 (6)	9111 (3)	6118 (3)	99 (10)	30 (3)	46 (4)	−3 (4)	10 (5)	6 (3)
C65	5238 (6)	9873 (3)	6698 (4)	123 (11)	35 (3)	63 (4)	−16 (5)	26 (5)	−3 (3)
C66	5450 (7)	9835 (4)	7696 (4)	173 (12)	36 (3)	63 (4)	−2 (5)	14 (6)	−14 (3)
C51	2524 (7)	5767 (3)	5815 (5)	182 (13)	28 (3)	71 (5)	−12 (5)	−3 (6)	−2 (3)
C52	3663 (8)	5860 (3)	5188 (4)	214 (14)	31 (3)	59 (4)	28 (5)	33 (6)	−4 (3)
C53	5274 (7)	6223 (4)	5719 (5)	118 (12)	32 (3)	100 (5)	31 (5)	18 (7)	−2 (3)
C54	5093 (8)	6335 (4)	6674 (5)	264 (17)	30 (3)	69 (5)	48 (6)	−46 (8)	−5 (3)
C55	3355 (8)	6060 (4)	6754 (4)	216 (14)	32 (3)	77 (5)	17 (5)	34 (7)	19 (3)

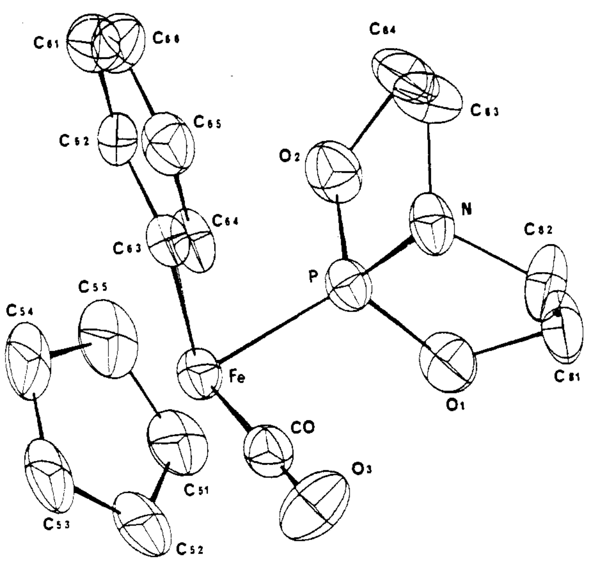

Figure 2. ORTEP representation and atomic numbering of **15b**.

for the Fe–P bond distance (2.105 Å), which is one of the shortest reported so far for an iron(II)–phosphane complex, the shortest previously reported being 2.122 Å in **30**,[25] and recently 2.102 Å in **28**.[26]

The considerable shortening of the Fe–P distance observed from **20** to **15b**, may originate from (i) the expected increase in s character of the phosphorus hybrid orbital binding iron due to the greater electronegativity of the phosphorus substituents in the bicyclic ligand **17**, (ii) a lessening of steric hindrance when PPh_3 (in **20**) is replaced by the much more compact bicyclic ligand **17**, and (iii) an increase in π-interaction between Fe and P (a high π-accepting capacity, higher than those of $P(OPh)_3$, $P(OCH_3)_3$, $P(OCH_2)_3CR$, or $P(CH_2CH_2CN)_3$ has indeed been found for ligands of type **17** in complexes with Mo(0) and W(0) on the basis of the ν_{CO} infrared data).[32,33] It is however not possible to evaluate the relative contributions of these effects in the measured Fe—P, Fe—C(Ph), Fe—C(Cp) and Fe—C(C≡O) bond lengths. It is also interesting to note that the last distance is one of the shortest Fe—C(C≡O) bond lengths known and, concomitantly, that the C≡O distance is very long (which also corresponds to a very low frequency of the ν_{CO} vibration), implying a higher order Fe—C bond than in any of the other compounds listed in Table IV, except **21**.

Table III. Selected Bond Lengths (Å) and Angles (deg)

	Bonds[a]		
Fe-P	2.105 (2)	P-N	1.692 (4)
Fe-CO	1.715 (5)	P-O1	1.620 (3)
Fe-C63	2.037 (5)	N-C82	1.468 (6)
Fe-C51	2.087 (5)	N-C83	1.473 (6)
Fe-C52	2.096 (5)	O1-C81	1.452 (5)
Fe-C53	2.107 (5)	O2-C84	1.473 (6)
Fe-C54	2.109 (5)	C81-C82	1.507 (7)
Fe-C55	2.111 (5)	C83-C84	1.504 (7)
CO-O3	1.162 (5)		
	Angles[b]		
P-Fe-CO	90.6 (2)	O2-P-N	97.1 (2)
C63-Fe-CO	94.5 (2)	P-N-C82	108.6 (3)
C63-Fe-P	83.9 (2)	P-N-C83	107.4 (3)
Fe-P-N	123.3 (2)	C82-N-C83	117.6 (4)
Fe-P-O1	114.5 (2)	Fe-CO-O3	178.5 (5)
Fe-P-O2	115.5 (2)	Fe-C63-C64	122.8 (4)
O1-P-O2	107.4 (2)	Fe-C63-C62	119.2 (4)
O1-P-N	96.1 (2)		

[a] C-C bond lengths: 1.359 (6)–1.402 (6) Å (av 1.388 Å) for the phenyl group; 1.382 (7)–1.436 (7) Å (av 1.408 Å) for the Cp ring. [b] Phenyl C-C-C bond angles: 117.9 (4)–122.6 (5)° (av 120.0°). Cp C-C-C bond angles: 105.3 (5)–109.3 (5)° (av 107.5°).

A second remarkable feature of the structure of **15b** is that the P–N bond is very short (1.69 Å) in spite of the fact that here the nitrogen atom is markedly pyramidal (sum of the angles around nitrogen is 333 ± 9.0°). It is comparable with bond distances found in aminophosphanes, in which the nitrogen atom adopts a planar configuration and for which it is customary to invoke a p_π–d_π contribution[34] (Me_2N-PCl_2 = 1.69 Å).[35] It is significantly

---

(25) Guggenberger, L. J.; Titus, D. D.; Flood, M. T.; Marsh, R. E.; Orio, A. A.; Gray, H. B. *J. Am. Chem. Soc.* **1972**, *94*, 1135.

(26) Reger, D. L.; Belmore, K. A.; Mintz, E.; Charles, N. G.; Griffith, E. A. H.; Amma, E. L. *Organometallics* **1983**, *2*, 101.

(27) Reisner, G. M.; Bernal, I.; Brunner, H.; Muschiol, M. *Inorg. Chem.* **1978**, *17*, 783.

(28) Andrianov, V. G.; Chapovskii, Yu. A.; Semion, V. A.; Struchkov, Yu. T. *J. Chem. Soc., Chem. Commun.* **1968**, 282.

(29) Burrow, M. I.; Sim, G. A.; Dobbie, R. C.; Mason, P. R. *J. Organomet. Chem.* **1974**, *69*, C4.

(30) Riley, P. E.; Davis, R. E., *Organometallics* **1983**, *2*, 286.

(31) Reger, D. L.; McElligott, P. J.; Charles, N. G.; Griffith, E. A. H.; Amma, E. L. *Organometallics* **1982**, *1*, 443.

(32) Febvay, J.; Grec, D.; Riess, J. G. *Inorg. Chem.* **1981**, *20*, 4285.

(33) Febvay, J.; Casabianca, F.; Riess, J. G. *J. Am. Chem. Soc.* **1984**, *106*, 7986. Febvay, J.; Casabianca, F.; Riess, J. G. *Inorg. Chem.* **1985**, *24*, 3235.

Table IV. Comparison of Bond Lengths (Å) and ν_{CO} Data (cm^{-1}) with Selected Literature Values

compd	no.	Fe—P	Fe—C(Ph)	⟨Fe—C(Cp)⟩	Fe—C(CO)	C≡O	ν_{CO}
η^5-CpFe(CO)[P(OCH$_2$CH$_2$)$_2$N](η^1-Ph)	**15b**	2.105 (3)	2.037 (5)	2.102 (11)	1.715 (5)	1.162 (5)	1930
η^5-CpFe(CO)(PPh$_3$)(η^1-Ph)[24]	**20**	2.23 (1)	2.11 (2)	2.14 (2)	1.78 (2)	1.18 (4)	1928
η^5-CpFe(CO)(PPh$_3$)CO$_2$(menthyl)[27]	**21**	2.214 (3)		2.113 (16)	1.670 (7)	1.206 (9)	1938
η^5-CpFe[P(OPh)$_3$]$_2$I[28]	**22**	2.15 (2)		2.10 (3)			
η^5-CpFe(CO)$_2$P(CF$_3$)$_2$[29]	**23**	2.265 (3)		2.097 (7)	1.768 (7)	1.138 (8)	2046, 2000
η^5-CpFe(CO)$_2$P(O)(CF$_3$)$_2$[29]	**24**	2.191 (3)		2.090 (7)	1.780 (7)	1.134 (7)	2062, 2019
η^5-CpFe(CO)$_3{}^{+}$[23]	**25**			2.070 (14)	1.816 (15)	1.112 (1)	2120, 2068
η^5-CpFe(CO)$_2$PPh$_3{}^{+}$[30]	**26**	2.242 (1)		2.093 (7)	1.771 (4)	1.139 (1)	2070, 2025
η^5-CpFe(CO)(dppe)$^{+}$[30]	**27**	2.209 (2)		2.094 (7)	1.774 (5)	1.138 (7)	1980
dppe = Ph$_2$PCH$_2$CH$_2$PPh$_2$		2.211 (2)					
η^5-CpFe(CO)[P(OPh)$_3$][η^1-(*Z*)-C(Me)=C(Ph)(Me)][26]	**28**	2.102 (2)	2.031 (8)	2.117 (23)	1.746 (7)	1.138 (9)	1951
η^5-CpFe(CO)[P(OPh)$_3$][η^1-C(CO$_2$Et)=CMe$_2$][31]	**29**	2.2236 (8)	2.030 (2)	2.117 (14)	1.724 (4)	1.149 (6)	1925
H$_2$Fe[PhP(OEt)$_2$]$_4$[25]	**30**	2.122					

shorter than the 1.75 Å found when N is coordinated to a BH$_3$ group in the bis(borane)bicycloaminophosphane **18**,[34] where no p_π–d_π contribution is expected for the P–N bond. This supports the idea that such a p_π–d_π interaction is responsible for the short P–N distance in **15b** and also shows that relationships between the P–N distances and bond angles around nitrogen should be used with caution.[36]

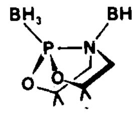

18

Mechanism. Although tertiary phosphanes have been extensively used as ligands in transition metal complex catalyzed reactions, the role of P–C bond breakage seems to have been long overlooked: P–C bond cleavage and formation of ortho-metalated species are, in part, responsible for the poisoning and decay of catalysts. Results on the decomposition of phosphanes under catalytic conditions are available now, and an increasing number of papers have reported transition-complex-promoted P–C bond scission.[37] Moreover, triarylphosphanes are now used as sources of aryl groups in synthetic chemistry.[37] When ortho-metalated species were recovered, it was at first speculated that these derivatives participated in aryl–P bond breaking; the ortho-metalation mechanism has however been ruled out by the use of para-substituted arylphosphanes. Two mechanisms are now proposed to explain the migration of aryl groups from phosphorus toward the metal: a 1,2-sigmatropic shift of the aryl group from the coordinated phosphane and an oxidative addition of the aryl–P bond on the metal.

The computed activation energy, calculated by Hoffmann,[38] for the symmetry-allowed 1,2-shift of a methyl group in the simplest H$_2$P(CH$_3$)–PdH$_3{}^-$ model is 23 kcal mol^{-1}; this barrier is reduced to a very low 1.6 kcal mol^{-1} for phenyl migration if the plane of the phenyl is perpendicular to the Pd–P axis; this barrier, although it may be underestimated, indicates that phenyl migration is accessible.[39] The obtention of stable binuclear or polynuclear μ-phosphido complexes of d^8 or d^9 (generally zerovalent) metals seems to favor the oxidative addition process. While the reaction is usually followed by reductive elimination of hydrocarbons, several others, producing dimers, trimers or other more complicated structures with aryl bridges or terminal aryls, are known.[37] The only sources of aryl groups are the phosphane ligands, which are cleft to give phosphido bridges.

All these studies deal however with phosphane complexes and not with phosphoranide adducts, for which the phenyl migration has been observed here. This leads to the question whether or not the phosphoranides play a more general role as intermediates in processes where P–C bond rupture is observed.

In the present study, an oxidative addition process can be ruled out since there is no change in oxidation state, either of iron or of phosphorus. The possibility of an ortho-metalation mechanism was ruled out by preparing and reacting the chemically labeled phosphoranide **13d**.

Under conditions similar to those described for **13b**, derivative **13d** is converted to **15d** (70% yield), whose ^{1}H NMR spectrum establishes the presence of a meta and para trimethyl-substituted phenyl group on the iron atom (CH$_3$ meta, 2.12 ppm, singlet; CH$_3$ para, 2.03 ppm, singlet; H ortho, 7.10 ppm, singlet), indicating that a 1,2-sigmatropic shift of the phenyl group has taken place. An ortho-metalation pathway would have yielded the ortho, meta, and para trimethyl-substituted phenyliron derivative **16**.

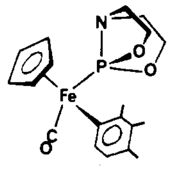

16

The quantitative recovery of the cationic iron derivative **11d** after the migration of the labeled phenyl group has been reversed establishes that it is the same carbon atom which is again bonded to phosphorus after migration.

The fact that the migration of the phenyl group back to phosphorus is quantitative implies a selective action of the acid. Treatment of η^5-CpFe(CO)(L)R (R = alkyl,[39] aryl[39a]) by the electrophile HE is known to result in the cleavage of the Fe–C bond and formation of RH and η^5-CpFe(CO)LE, and it has been shown that σ-aryliron derivatives are much more reactive than σ-alkyliron compounds toward HE.[39a] Furthermore, the action of an acid HX on aminophosphanes, even when complexed on a metal, generally results in the hydrolysis of the P–N bond.[40] Riess et al. have however shown that the bicyclic aminophosphane **17**, in which the nitrogen atom is forced to a pyramidal configuration by the constraining bicyclic system, is an exception to this rule; its nitrogen displays a definite basic character, as illustrated by the isolation of the diborano adduct **18**[34] and of the stable protonated derivative **19**(H$^+$).[33] These observations lead us to propose that the nucleophilic center in **15b,d** is located on nitrogen and not on iron or on the Fe–phenyl bond.

The nitrogen atom in **15b,d** is expected to have a comparably strong basic character, as in **19**, and its protonation will result in the, here unstable, adduct **15**(H$^+$) in which the electrophilic

---

(34) Grec, D.; Hubert-Pfalzgraf, L. G.; Riess, J. G.; Grand, A. *J. Am. Chem. Soc.* **1980**, *102*, 7133. Grec, D.; Hubert-Pfalzgraf, L. G.; Riess, J. G.; Grand, A. *Inorg. Chem.* **1985**, *24*, 4642.

(35) Corbridge, D. E. C. *The Structural Chemistry of Phosphorus*; Elsevier: Amsterdam, 1974; p 289.

(36) Dupart, J. M.; Grand, A.; Pace, S.; Riess, J. G. *Inorg. Chem.* **1984**, *23*, 3776.

(37) Garrou, P. E. *Chem. Rev.* **1985**, *85*, 171 and references therein.

(38) Ortiz, J. V.; Havlas, Z.; Hoffmann, R. *Helv. Chim. Acta* **1984**, *67*, 1.

(39) (a) De Luca, N.; Wojcicki, A. *J. Organomet. Chem.* **1980**, *193*, 359. (b) Rogers, W. N.; Page, J. A.; Baird, M. C. *Inorg. Chem.* **1981**, *20*, 3521.

(40) Ellis, J. E. *J. Organomet. Chem.* **1976**, *111*, 331.

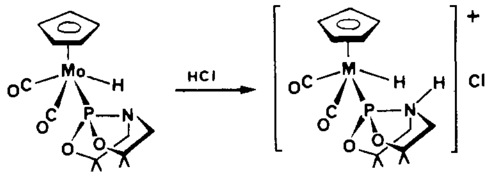

19 **19**(H^+)

character of the phosphorus atom is increased. If a group suitable for migration, like the phenyl group, is present on the metal center, a concerted redistribution of bonds can occur. The stability of the protonated adducts **19**(H^+) when compared to **15**(H^+), is thus likely to arise from the absence of a suitable migrating group.

It should be noted that the rearrangement observed here, which can be reversed quantitatively, where no change in oxidation state occurs for iron or phosphorus, definitely differs from the irreversible transfer of a phenyl group (i) from a phosphonium ion to iron, as observed by Ellis,[40] (ii) from a phosphorus ylide to nickel, as reported by Keim et al.[41] or (iii) from triphenylvinylphosphonium bromide to the α-carbon of the vinyl group under alkaline hydrolysis, where a phosphane oxide is obtained.[42] Nor is it related to the reversible oxidative addition of PPh_3 to zerovalent Ni and Pd complexes observed by Fahey and Mahan,[43] which constitutes one of the few examples of a phenyl group migration from a metal center to phosphorus:[50] treating $Ni^{II}(Ph)(PEt_3)_2(Br)$ with $LiPPh_2$ leads to $Ni(PEt_3)_3PPh_3$ in low yield (20%). More recently, the migration of an allylic group from palladium to phosphorus has been reported.[44]

Investigations were undertaken in order to explore the extent of the migration phenomenon reported here. Complex reactions were observed when the phenyl group was replaced by methyl, benzyl, and vinyl groups, while the allyl group underwent migration from the phosphorus to the iron atom, but with simultaneous rearrangement into a vinyl group.[45] This transformation, which also occurs via a phosphoranide adduct, is the result of a C–H activation process followed by a P–C bond rupture.

Furthermore, this reversible migration of a phenyl group appears so far to be specific to iron; the ruthenium phosphoranide **13** decomposes rapidly upon heating at 30 °C in THF, but no phenylruthenium compound could be detected by IR or ^1H and ^{31}P NMR spectroscopy. The Mo and W phosphoranides are much more stable, since slow decomposition occurs only under prolonged heating and no phenyl–metal bonds appear to form under these conditions. This specificity is, at present, not well understood. The lesser stability of the iron phosphoranide compared to the analogous Mo and W derivatives may perhaps be accounted for by the differences in their atomic sizes (Fe^{II} = 1.23 Å; Ru^{II} = 1.33 Å; Mo^{II} = 1.39 Å; W^{II} = 1.41 Å)[46] resulting in a greater strain in the $\overline{\text{M–N–P}}$ or $\overline{\text{M–O–P}}$ metallacycles for iron than for Ru, Mo, or W. The possible existence, in the case of iron only, of a phosphoranide adduct **14′**, in which the metal is coordinatively and electronically unsaturated, could be of importance in regard to these differences in behavior. However, this size effect should not prevent the obtention of the iron amido–phosphane adduct analogous to **5**, but this was not even detected. On the other hand, many stable Ru and W σ-phenyl derivatives analogous to **15** are known,[16c] while only one stable complex in the case of Mo has been reported so far.[46]

Conclusions

Our results further illustrate the exceptional versatility of the cyclic P/N phosphorane **1** and phosphane ligand **17**. **1** is shown here to be able to coordinate transition metals in its tautomeric open form, (i) through phosphorus alone or (ii) through both phosphorus and nitrogen and, after proton abstraction, (iii) as a phosphane and amide monocyclic ligand and (iv) through both phosphorus and nitrogen (or oxygen) in its closed bicyclic form. In the latter situation, **1** thus acts as a phosphoranide ligand in which phosphorus is in the formal oxidation state +3. A most surprising new behavior of this ligand and of **17** is a reversible nitrogen-assisted migration of the phenyl group between phosphorus and iron.

The Ru derivative **11c** under the action of a base behaves differently from the Fe analogues **11b**,**d**. While only the phosphoranide adduct is detected for Fe, the abstraction of H on nitrogen results in the formation of an amide that is transformed to a phosphoranide for Ru, as for Mo and W.

The iron phenylphosphoranides, and these only, convert into the phenyliron complexes **15b**,**d**. That these transformations can be reversed quantitatively under the action of an acid is even more surprising. Chemical labeling of the phenyl ring established that it is the same carbon atom that is alternately bonded to phosphorus or to iron, establishing a 1,2-sigmatropic shift mechanism for this phenyl migration.

Finally, these results show that the possible intermediate formation of phosphoranide adducts should be taken into account when discussing the mechanism of P–C bond rupture. From the point of view of phosphorus chemistry, the reversible phenyl migration exemplifies a metal-induced interconversion between a hypervalent P(V) phosphorane and a trivalent P(III) phosphane derivative.

Experimental Section

All the reactions were carried out under dry oxygen-free argon. All solvents were freshly distilled under argon from appropriate drying agents. ^1H, ^{13}C, and ^{31}P NMR spectra were recorded on a Bruker WH-90 spectrometer. Chemical shifts are given in ppm downfield from internal Me_4Si for the ^1H and ^{13}C shifts and from external H_3PO_4 for the ^{31}P shifts. Infrared spectra were obtained for KBr disks on a Perkin-Elmer 577 grating spectrophotometer. Elemental analyses were performed by the Service Central de Microanalyses of the CNRS, France. Phosphoranes **1**,[51] η^5-$CpFe(CO)_2$ (X = Cl, Br),[52] and η^5-$CpRu(CO)_2Cl$[53] were prepared according to published procedures.

Preparation of 8a, 9a, and 10a. A mixture of 2.4 g (9.34 mmol) of η^5-$CpFe(CO)_2Br$ with 2.0 g (9.48 mmol) of phosphorane **1** in 200 mL of THF was stirred at room temperature for 2 days. A cream-colored precipitate formed, which was isolated by filtration, washed with THF (3 × 40 mL), and dried under vacuum to give 2.8 g (6 mmol) of hygroscopic **8a** (65%), soluble in CH_2Cl_2, acetone, and acetonitrile and insoluble in EtOH, ether, and pentane. Anal. Calcd for $C_{17}H_{19}BrFeNO_4P\cdot{}^1/_2H_2O$ (M_r = 476.8): C, 42.7; H, 4.2; N, 2.93; P, 6.50; Fe, 11.70. Found: C, 42.7; H, 3.93; N, 2.79; P, 6.35; Fe, 11.74. IR (KBr): ν_{CO} = 2050, 2000 cm^{-1}; ν_{NH} = 3400 cm^{-1}. $\delta(^{31}P)$ (CH_2Cl_2) = 180.

The above THF fractions were collected and evaporated, leaving an oily residue, which was dissolved in toluene. The solution was filtered, and the solvent was removed under vacuum. The residue was washed with ether, leaving 1.5 g (3.4 mmol) of a dark brown powder consisting of **10a** (30%) soluble in CH_2Cl_2, THF, acetone, acetonitrile, and toluene and insoluble in ether and pentane. Anal. Calcd for $C_{16}H_{19}BrFeNO_3P$ (M_r = 439.8): C, 43.65; H, 4.32; N, 3.18; P, 7.05. Found: C, 44.11; H, 4.34; N, 3.10; P, 6.93. IR (KBr): ν_{CO} = 1940 cm^{-1}; ν_{NH} = 3320 cm^{-1}. $\delta(^{31}P)$ (CH_2Cl_2) = 210.4 for **10a** (40%) and 195.7 for **9a** (60%). $\delta(^1H)$ (CH_2Cl_2) = 5.0 for the Cp of **10a** (d, $^3J_{HP}$ = 1.5 Hz, 40%) and 4.50 for the Cp of **9a** (d, $^3J_{HP}$ = 1.5 Hz, 60%).

Preparation of 8b and 10b. The same experimental procedure when applied to 1.9 g (8.96 mmol) of η^5-$CpFe(CO)_2Cl$ gave 2.30 g (60%) of

---

(41) Keim, W.; Kowalt, F. M.; Guiger, C.; Goddard, R. *Angew. Chem., Int. Ed. Engl.* **1978**, *17*, 466.

(42) Shutt, J. R.; Trippett, S. *J. Chem. Soc.* **1959**, 705.

(43) Fahey, D.; Mahan, J. E. *J. Am. Chem. Soc.* **1976**, *98*, 4499.

(44) Goel, A. B. *Tetrahedron* **1984**, *25*, 4599.

(45) Vierling, P.; Riess, J. G. *J. Am. Chem. Soc.* **1984**, *106*, 2432.

(46) Pauling, L. *The Nature of the Chemical Bond*, 3rd ed.; Cornell University Press: Ithaca, NY, 1960; p 249.

(47) Nesmeyanov, A. N.; Makanova, L. G.; Ustynyuk, N. A. *J. Organomet. Chem.* **1970**, *23*, 517.

(48) Busing, W. R.; Martin, K. U.; Levy, H. A. *ORXFLS3*, Report ORNL 59/4/37; Oak Ridge National Laboratory: Oak Ridge, TN, 1971.

(49) *International Tables for X-Ray Crystallography*; Kynoch: Birmingham, England, 1974; Vol. IV.

(50) For other examples of a phenyl migration from Ni to P, see: Cassar, L.; Foa, M. *J. Organometal. Chem.* **1974**, *74*, 75.

(51) Houalla, D.; Mouheich, T.; Sanchez, M.; Wolf, R. *Phosphorus* **1975**, *5*, 229.

(52) Fischer, E. O.; Moser, E. *Inorg. Synth.* **1970**, *12*, 35.

(53) Blackmore, T.; Cotton, J. D.; Bruce, M. I.; Stone, F. G. A. *J. Chem. Soc. A* **1968**, 2931.

8b (hygroscopic) and 1.25 g (35%) of **10b**. **8b**. Anal. Calcd for $C_{17}H_{19}ClFeNO_4P,H_2O$ (M_r = 441.4): C, 46.22; H, 4.75; N, 3.17. Found: C, 46.54; H, 4.36; N, 3.20. $\delta(^{31}P)$ (CH_2Cl_2) = 180. IR (KBr): ν_{CO} = 2050, 2000 cm^{-1}; ν_{NH} = 3400 cm^{-1}. **10b**. Anal. Calcd for $C_{16}H_{19}ClFeNO_3P$ (M_r = 395.4): C, 48.55; H, 4.80; N, 3.54. Found: C, 48.50; H, 4.78; N, 3.47. IR (KBr): ν_{CO} = 1940 cm^{-1}; ν_{NH} = 3300 cm^{-1}. This compound was further characterized in the form of its PF_6^- or BPh_4^- salt (see below).

Preparation of 11a,b from 10a,b. A 1.3-g (2.9-mmol) sample of **10a** (or a 1.2-g (2.95-mmol) sample of **10b**) was dissolved in 60 mL of ethanol and heated to 60 °C. 900 mg (5.5 mmol) of NH_4PF_6 dissolved in 60 mL of water were then added under stirring. An orange precipitate appeared. The solution was stirred for 1 day at room temperature. To complete precipitation, a further amount of NH_4PF_6 (500 mg in 60 mL of water) was added. After 4 h, the solution was cooled to 3–5 °C. The precipitate was isolated by filtration, carefully washed with ice-cold water (the product is slightly soluble in water) and ether, and then dried, to give 1.1 g (2.18 mmol) (74%) of an orange powder consisting of **11a**. Anal. Calcd for $C_{16}H_{19}F_6FeNO_3P_2\cdot{}^1/_2H_2O$ (M_r = 513.8): C, 37.43; H, 3.89; N, 2.72; P, 12.06; F, 22.18. Found: C, 37.46; H, 3.83; N, 2.74; P, 12.15; F, 22.01. $\delta(^{31}P)$ (acetone) = 208.6 and −144.8 (PF_6^- septuplet). $\delta(^1H)$ (acetone-d_6) = 5.15 (d, $^3J_{HP}$ = 1.2 Hz, Cp) (4.90 in CD_3CN). IR (KBr): ν_{CO} = 1975 cm^{-1}; ν_{NH} = 3300 cm^{-1}.

The same procedure applied to 1.3 g (2.95 mmol) of **10a** (or to 1.2 g (2.95 mmol) of **10b**) and to 5 mmol of $NaBPh_4$ afforded 1.8 g of an orange powder consisting of **11b** (90%). $\delta(^{31}P)$ (CH_3CN) = 208.8. $\delta(^1H)$ (CD_3CN) = 4.85 (d, $^3J_{HP}$ = 1.2 Hz, Cp). IR (KBr): ν_{CO} = 1960 cm^{-1}; ν_{NH} 3240 cm^{-1}; $\nu_{C=C}$ = 1580 cm^{-1} (BPh_4^-).

Preparation of 11d from 2 and CpFe(CO)₂Br. The same experimental procedure as used for **8a** and **10a**, when applied to 1.48 g (5.76 mmol) of η^5-$CpFe(CO)_2Br$ and 1.57 g (6.2 mmol) of **2**, gave 1.8 g (60%) of **8d** and 0.33 g (12%) of **10d**, which was quantitatively converted to **11d** (0.45 g, 90%) by using the same procedure as for the preparation of **11b**. **8d**. IR (KBr): ν_{CO} = 2050 cm^{-1}, 2000 cm^{-1}; ν_{NH} = 3300 cm^{-1}. **11d**. Anal. Calcd for $C_{43}H_{45}BFeNO_3P,H_2O$ (M_r = 738.6): C, 69.86; H, 6.36; N, 1.89; P, 4.20. Found: C, 70.11; H, 6.50; N, 1.82; P, 4.30. $\delta(^{31}P)$ (acetone) = 208.4. $\delta(^1H)$ (CD_3CN) = 4.82 (d, $^3J_{HP}$ = 1.5 Hz, 5 H, Cp), 2.38 (s, 6 H, CH_3 meta), and 2.27 (s, 3 H, CH_3 para). IR (KBr): ν_{CO} = 1965 cm^{-1}; ν_{NH} = 3220 cm^{-1}; $\nu_{C=C}$ = 1580 cm^{-1} (BPh_4^-).

Conversion of 8a,b and 8d to 11b and 11d, Respectively. A solution of 3.0 g (6.4 mmol) of **8a** (or 2.7 g (6.4 mmol) of **8b**) in CH_2Cl_2 was added to a solution of $NaBPh_4$ (6.5 g, 19 mmol) in EtOH and stirred for 4 h. A second amount of $NaBPh_4$ (1 g, 3 mmol) and 40 mL of water were added, and the solution was stirred for 1 h. The organic layer was separated, washed with 3 × 50 mL of water, and evaporated, and the residue was dried under vacuum. The solid was redissolved in CH_2Cl_2 (100 mL) and the solution exposed to UV irradiation (HP 125-W lamp) for 5 h, after which all the starting material had disappeared, as shown by infrared monitoring. The solvent was removed and the residue dissolved in 20 mL of THF and cooled to −30 °C. The orange precipitate was isolated by filtration and washed with THF and ether to give 1.3 g (1.90 mmol; 30%) of **11b**. The same experimental procedure applied to 3 g (5.9 mmol) of **8d** afforded 2.12 g (2.95 mmol; 50%) of **11d**.

Preparation of 15b or 15d. A solution of LiMe (1.6 M) in ether (0.7 mL) was added dropwise under stirring to a solution of 410 mg (0.8 mmol) of **11b** (or **11a**) in 20 mL of THF at −80 °C. After the mixture was heated at 60 °C for 4 h, the solvent was removed under vacuum and the residue redissolved in 30 mL of ether. This solution was purified by chromatography on neutral, activated silica (h = 3 cm, o.d. = 2 cm) with ether as eluant, until the effluent was colorless. The solution was concentrated and cooled to −30 °C, affording 100 mg (0.2 mmol; 35%) of **15b** as amber-colored crystals. Anal. Calcd for $C_{16}H_{18}FeNO_3P$ (M_r = 358.8): C, 53.50; H, 5.00; N, 3.90. Found: C, 53.45; H, 5.14; N, 3.78. IR (KBr): ν_{CO} = 1920 cm^{-1}; $\nu_{C=C}$ = 1560 cm^{-1} (fine, phenyl). $\delta(^{31}P)$ (THF) = 217. $\delta(^1H)$ (CD_2Cl_2) = 7.50 (m, 2 H, meta), 6.80 (m, 3 H, ortho + para), 4.69 (d, $^3J_{HP}$ = 0.9 Hz, 5 H, Cp), 3.78 (m, 4 H, $OC\mathit{H}$), and 2.90 (m, 4 H, $NC\mathit{H}_2$). $\delta(^{13}C)$ ($CDCl_3$) = 215 (CO), 149 (s, 2 C, ortho or meta), 128.6 (s, 2 C, ortho or meta), 124 (s, 1 C, para); 86 (s, Cp), 71.8 (d, OCH_2), 71.6 (d, OCH_2), 56.3 (d, $NC\mathit{H}_2$), and 56.1 (d, NCH_2); $^2J_{CP}$ ~ 2 Hz for all doublets. The same experimental procedure applied to 500 mg (0.69 mmol) of **11d** yielded 200 mg (0.5 mmol; 72%) of **15d**. Anal. Calcd for $C_{19}H_{24}FeNO_3P$ (M_r = 400.8): C, 56.88; H, 5.99; N, 3.49. Found: C, 56.52; H, 5.95; N, 3.29. IR (KBr): ν_{CO} = 1920 cm^{-1}; $\nu_{C=C}$ = 1560 cm^{-1} (phenyl). $\delta(^{31}P)$ (THF) = 217. $\delta(^1H)$ (CD_2Cl_2) = 7.1 (s, 2 H, ortho), 4.63 (d, $^3J_{HP}$ = 0.9 Hz, 5 H, Cp), 3.80 (m, 4 H, OCH_2), 3.05 (m, 4 H, NCH_2), 2.12 (s, 6 H, CH_3 meta), and 2.03 (s, 3 H, CH_3 para).

Reaction of Gaseous HCl with 15b and 15d. Dry gaseous HCl was bubbled through a solution of 80 mg (0.22 mmol) of **15b** (or 80 mg (0.2 mmol) of **15d**) in THF. The solution turned immediately from yellow to dark red. The solvent was then removed, leaving a dark red powder, which was identified as $[\eta^5\text{-}CpFe(CO)(Cl)RP(OCH_2CH_2)_2NH_2^+]Cl^-$. To a solution of this powder in ethanol were then added 1 equiv of NEt_3 and 3 equiv of $NaBPh_4$ in 10 mL of water. An orange precipitate was formed, which was isolated by filtration, washed with water and ether, and dried under vacuum to give a compound whose spectral characteristics are identical with those of the independently prepared **11b** (or **11d**) (150 mg, ~ 100% starting from **15b**; 145 mg, ~100% starting from **15d**).

Preparation of 10c. A 500-mg (1.9-mmol) sample of η^5-$CpRu(CO)_2Cl$ and 410 mg (1.95 mmol) of **1** were dissolved in 30 mL of THF, and the solution was refluxed for 3 h until all the starting material had disappeared (as shown by IR monitoring). The ν_{CO} vibrations of the starting complex at 2060 and 1995 cm^{-1} were then replaced by a single ν_{CO} absorption at 1965 cm^{-1}. The solvent was then removed under vacuum and the yellow residue washed with ether to give 800 mg (1.82 mmol) of a pale yellow powder of **10c** (94%). Orange crystals were obtained by recrystallization from THF. **10c** is moderately soluble in $CHCl_3$, CH_2Cl_2, acetone, acetonitrile, ethanol, and THF. Anal. Calcd for $C_{16}H_{19}ClNO_3PRu$ (M_r = 441.3): C, 43.51; H, 4.31; N, 3.17. Found: C, 43.78; H, 4.40; N, 3.19. IR (KBr): ν_{CO} = 1945 cm^{-1} (1970 cm^{-1} in $CHCl_3$); ν_{NH} = 3320 cm^{-1}. $\delta(^{31}P)$ ($CDCl_3$) = 183 for **10c** (35%) and 167.5 for **9c** (65%). $\delta(^1H)$ ($CDCl_3$) = 5.44 (d, $^3J_{HP}$ = 0.6 Hz, Cp of **10c**, 35%) and 5.00 (d, $^3J_{HP}$ = 0.9 Hz, Cp of **9c**, 65%).

Preparation of 11c. The experimental X^-/BPh_4^- anion-exchange procedure applied to 3.55 g (8 mmol) of **10c** gave 5.3 g (90%) of the pale yellow microcrystalline compound **11c**. Pale yellow crystals were obtained by recrystallization from CH_3CN. **11c** is sparingly soluble in CH_3CN and acetone and insoluble in $CHCl_3$, CH_2Cl_2, ethanol, and ether. Anal. Calcd for $C_{40}H_{39}BNO_3PRu$ (M_r = 724.56): C, 66.25; H, 5.38; N, 1.93. Found: C, 66.34; H, 5.43; N, 2.03. IR (KBr): ν_{CO} = 1975 cm^{-1}; ν_{NH} = 3240 cm^{-1}; $\delta(^{31}P)$ (CH_3CN) = 182. $\delta(^1H)$ (CD_3CN): 5.32 (d, $^3J_{HP}$ = 0.6 Hz, Cp).

Preparation of 12c or 13c. A solution of 1.1 equiv of LiMe in ether (1.6 M) was slowly added under stirring to a solution of 3 g (2.76 mmol) of **11c** in 30 mL of THF at −80 °C. Then 30 mL of ether was added, and the solution was kept at −30 °C for 2 days and then cooled to −70 °C. The $LiBPh_4$ that precipitated was filtered and washed with 2 × 10 mL of ether. The combined solutions were evaporated, and the solid residue was washed with pentane (2 × 10 mL) (during this washing step, the pale yellow powder turned to yellow-orange) and dried under vacuum, to give 1.07 g (95%) of **12c** or **13c**, as an orange-yellow powder, which was recrystallized from THF/pentane (1/5) at −30 °C, leaving orange-red crystals. Anal. Calcd for $C_{16}H_{18}NO_3PRu$ (M_r = 404.76): C, 47.43; H, 4.45; N, 3.46; P, 7.66. Found: C, 47.50; H, 4.60; N, 3.34; P, 7.46. IR (KBr): ν_{CO} = 1920 cm^{-1}. $\delta(^{31}P)$ (THF) = 69. $\delta(^1H)$ (CD_2Cl_2, −40 °C) = 5.15 (s, Cp). At room temperature the compound reacts with CD_2Cl_2 and converts to **10c** and **9c**.

X-ray Studies for 15b

Data Collection and Reduction. Amber crystals of **15b** suitable for X-ray work were obtained by slow crystallization at −30 °C in a 1/1 pentane/ether mixture. A crystal with approximate dimensions of 0.15 × 0.15 × 0.2 mm was mounted in a capillary under an atmosphere of nitrogen and was used for preliminary investigations and data collection. From Weissenberg photographs, the space group was assumed to be $P2_1/n$ (systematic absences: $h0l$ for $h + l$ odd, $0k0$ for k odd). The unit cell parameters were refined by a least-squares fitting based on the angular position of 25 reflections. The results are summarized in Table I, where the conditions for data collection are also listed. The intensity of 2846 independent reflections ($2° < \theta < 25°$) were collected on an automatic ENRAF-NONIUS CAD-4 diffractometer using graphite monochromated Mo Kα radiation, and ω-scan mode. The intensities of three standard reflections ($\bar{2}\bar{7}\bar{5}$, $\bar{4}36$, $4\bar{3}\bar{6}$) were recorded periodically, and no decrease was observed during the data collection. The data were corrected for Lorentz and polarization effects but not for absorption.

Solution and Refinement of the Structure. The structure was solved by the heavy-atom method. The Harker section of the Patterson function showed clearly the iron atom at 0.32, 0.72, 0.58. The remaining nonhydrogen atoms were located in successive Fourier syntheses. The refinement using XFLSN[48] was based on 2000 reflections ($F_o \geq 2.5\sigma(F_o)$) with isotropic thermal parameters for non-hydrogen atoms. Anomalous dispersion effects were included for the iron atom, the values of $\Delta f'$ and $\Delta f''$ were taken from ref 49. The R factor reached the values of R_w = 0.056, R = 0.073 ($R_w = (\sum_w|F_o - F_c|^2/\sum_w F_o^2)^{1/2}$ and $R = \sum|F_o - F_c|/\sum F_o$). At this stage of refinement, all hydrogen atoms were located by a Fourier difference synthesis. They were included in the final refinement with isotropic thermal factors fixed at 6.0 Å.^{2}

Finally, the R factors converged to R_w = 0.035, R = 0.057. Final atomic coordinates and anisotropic thermal parameters with their estimated standard deviations are listed in Table II; bond lengths and bond angles are listed in Table III.

Registry No. **1**, 57680-64-5; **2**, 57671-89-3; **8a**, 104489-87-4; **8b**, 104489-84-1; **8d**, 104489-95-4; **9c**, 104489-88-5; **10a**, 104489-89-6; **10b**, 104489-85-2; **10c**, 104489-92-1; **10d**, 104505-66-0; **11a**, 77681-64-2; **11b**, 104489-86-3; **11c**, 104505-65-9; **11d**, 104489-94-3; **12c**, 104489-90-9; **13d**, 104531-45-5; **15b**, 77659-95-1; **15d**, 104489-91-0; η^5-CpFeCO$_2$Br, 12078-20-5; η^5-CpFeCO$_2$Cl, 12107-04-9; η^5-CpRuCO$_2$Cl, 32611-12-4.

Supplementary Material Available: Table V, least-squares planes, and Table VI, atomic coordinates for hydrogen atoms (2 pages); listing of observed and calculated structure factors (11 pages). Ordering information is given on any current masthead page.

Contribution from the Department of Chemistry and Biochemistry,
University of Colorado, Boulder, Colorado 80309

Syntheses of Secondary-Amine-Substituted Bis(phosphino) Molybdenum Tetracarbonyl Complexes

Abbas Tarassoli,[1a] Haw-Jan Chen,[1b] Martin L. Thompson,[1c] Viloya S. Allured, R. Curtis Haltiwanger, and Arlan D. Norman*

Received April 3, 1986

Reaction of PhN(PCl$_2$)$_2$, PhN[P(NHPh)$_2$]$_2$, or the 1,3,2,4-diazadiphosphetidines [(PhNH)PNPh]$_3$ and [(PhNH)P$_2$(NPh)$_2$]$_2$NPh with norbornadiene-Mo(CO)$_4$ yields the cis complexes PhN(PCl$_2$)$_2$Mo(CO)$_4$ (**5**), PhN[P(NHPh)$_2$]$_2$Mo(CO)$_4$ (**6**), [(PhNH)PNPh]$_3$Mo(CO)$_4$ (**7**), and [(PhNH)P$_2$(NPh)$_2$]$_2$NPhMo(CO)$_4$ (**8**) in high yields. Reactions of nor·Mo(CO)$_4$ with PhN[P(NHPh)$_2$]$_2$ or a PhN[P(NHPh)$_2$]$_2$-(PhNH)$_3$P mixture or (PCl$_3$)$_2$Mo(CO)$_4$ with PhNH$_2$/Et$_3$N yields **6** quantitatively, in reactions that involve metal-templated P-N bond condensation reactions. **5** reacts with PhNH$_2$/Et$_3$N or *i*-PrNH$_2$/Et$_3$N to form **6** or *i*-PrN[(*i*-PrNH)$_3$(PhNH)P$_2$]Mo(CO)$_4$ (**9**), respectively. **6** has been characterized structurally by single-crystal X-ray crystallography. Crystals of $6\cdot{}^1/_2$C$_6$H$_6$ are hexagonal, space group $P6_122$, with a = 15.604 (4) Å, b = 15.604 (4) Å, c = 28.712 (4) Å, and Z = 6. The structure, solved by direct methods, refined to R = 0.074 and R_w = 0.085 for 539 observed reflections. The complex is a bis(phosphino)amino complex in which phosphorus atoms are coordinated to cis positions of the Mo(CO)$_4$ moiety. Comparison of physical and spectral properties of **5**, **7**, **8**, and **9** with those of **6** allows the former compounds to be characterized as bis(phosphino)amine complexes. In every case bis(phosphino) phosphorus coordination to the Mo(CO)$_4$ moiety occurs; no evidence for 1,3,2,4-diazadiphosphetidine terminal phosphorus or ring coordination is seen. Reaction of *cis*-(PhNPCl)$_2$ or *cis*-[(PhNH)PNPh]$_2$ with nor·Mo(CO)$_4$ yields intractable products.

Introduction

Recently, we reported the preparation and structural characterization of the secondary-amino- and 1,3,2,4-diazadiphosphetidinyl-substituted bis(phosphino)amines **1**–**3**.[2-6] Because they are phosphorus(III) compounds that contain N-H bonds and a P$_2$N$_2$ ring functionality, they are potentially valuable intermediates for the synthesis of novel bis(phosphino)amine-metal complexes, heteroatom-substituted phosphorus-nitrogen ring compounds, and new phosphorus-nitrogen polymers. The chemistry of **1**–**3** is so far largely unexplored; however, it is known that they are relatively labile; e.g., **1** undergoes aniline elimination and ring closure to [(PhNH)PNPh]$_2$ (**4**) (eq 1)[6,7] and **2** undergoes oligomer interconversion to a mixture of **4** and **2**.[3,6] Consequently, there may be advantages to stabilizing compounds such as **1**–**3** by their coordination to metal centers.

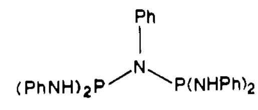

1

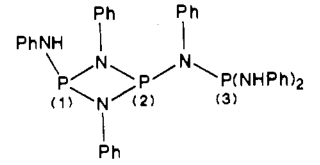

2

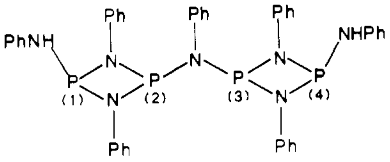

3

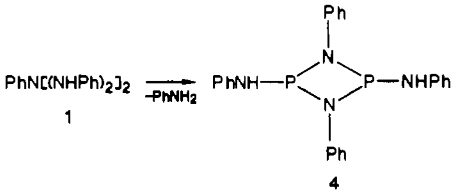

(1)

$$\underset{\mathbf{2}}{2[(\text{PhNH})\text{PNPh}]_3} \rightleftharpoons \underset{\mathbf{4}}{3[(\text{PhNH})\text{PNPh}]_2} \qquad (2)$$

In order to more fully develop the chemistry of amine-substituted phosphines such as **1**–**4**, we have undertaken a study of their coordination properties and syntheses on metal moiety centers. We have sought to stabilize the aminophosphines and subsequently develop routes to otherwise inaccessible systems. in addition, since metal coordination of 1,3,2,4-diazadiphosphetidine ring systems has been studied only slightly,[8-11] their coordination characteristics toward metals continue to be of interest. A preliminary report of the synthesis of PhN[P(NHPh)$_2$]$_2$Mo(CO)$_4$ has been published.[12]

---

(1) Permanent addresses: (a) Shahid Chamran University, Ahwaz, Iran. (b) Institute of Nuclear Energy Research, Lung-Tan, Taiwan. (c) Lake Forest College, Lake Forest, IL 60045.

(2) Thompson, M. L.; Haltiwanger, R. C.; Norman, A. D. *J. Chem. Soc., Chem. Commun.* **1979**, 647.

(3) Thompson, M. L.; Tarassoli, A. T.; Haltiwanger, R. C.; Norman, A. D. *J. Am. Chem. Soc.* **1981**, *103*, 6770.

(4) Thompson, M. L.; Tarassoli, A.; Haltiwanger, R. C.; Norman, A. D., submitted for publication.

(5) Tarassoli, A.; Haltiwanger, R. C.; Norman, A. D. *Inorg. Chem.* **1982**, *21*, 2684.

(6) Tarassoli, A.; Thompson, M. L.; Hill, T. G.; Norman, A. D., submitted for publication.

(7) Trishin, Y. G.; Chistokletov, V. N.; Kosovtev, V. V.; Petrov, A. A. *Zh. Org. Khim.* **1975**, *11*, 1752.

(8) Zeiss, W.; Feldt, C. H. *J. Organomet. Chem.* **1977**, *127*, C5.

(9) (a) Hawker, P. N.; Jenkins, L. S.; Willey, G. R. *J. Organomet. Chem.* **1976**, *118*, C44. (b) Jenkins, L. S.; Willey, G. R. *J. Chem. Soc., Dalton Trans.* **1979**, 777.

(10) Maisch, H. *Z. Naturforsch., B: Anorg. Chem. Org. Chem.* **1979**, *34B*, 784.

(11) Burckett St. Laurent, J. C. T. R.; Hosseini, H. E.; Sinclair, J.; Nixon, J. E. *Inorg. Chim. Acta* **1980**, *44*, L17.

(12) Chen, H.-J.; Tarassoli, A.; Haltiwanger, R. C.; Allured, V. S.; Norman, A. D. *Inorg. Chim. Acta* **1982**, *65*, L69.

0020-1669/86/1325-4152$01.50/0